Chelator-Induced Disappearance of Carboxylate Stretching Vibrational Modes in S_2/S_1 FTIR Spectrum in Oxygen-Evolving Complex of Photosystem II†

Yukihiro Kimura* and Taka-aki Ono*

Laboratory for Photo-Biology(1), RIKEN Photodynamics Research Center, The Institute of Physical and Chemical Research, 519-1399 Aoba, Aramaki, Aoba, Sendai 980-0845, Japan

Received June 12, 2001; Revised Manuscript Received August 20, 2001

ABSTRACT: Fourier transform infrared (FTIR) spectroscopy has been applied toward studies of photosynthetic oxygen evolution, especially on the effects of Ca^{2+} depletion and chelating agents using S_2/S_1 FTIR difference spectrum in the mid-IR region. Ca^{2+} depletion showed little influences on the symmetric (1365/1404 cm^{-1}) and the asymmetric (1587/1562 cm^{-1}) stretching bands of a carboxylate, which are typical of the S_2/S_1 vibrational features induced by the oxidation of the Mn-cluster; however, minor changes were observed in the amide regions. Addition of a chelating agent (EDTA or EGTA) to the Ca^{2+}-depleted membranes resulted in the disappearance of the carboxylate bands concurrent with large modifications of the amide bands with an apparent K_d value of approximately 0.49 mM (for EDTA). The carboxylate bands and the greater part of the amide bands were restored by the replenishment of $CaCl_2$, and the chelators did not affect the spectrum in the nondepleted control membranes, indicating that the effects of the chelator are reversible and manifest only in the cases in which the Ca^{2+} site is unoccupied by Ca^{2+}. Ca^{2+}-depleted membranes showed the normal $S_2Q_A^-$ thermoluminescence band, and further addition of EDTA did not show any effects on the peak temperature and peak intensity. Moreover, the Ca^{2+}-depleted membranes in the presence of EDTA exhibited the S_2 multiline EPR signal with nearly the normal hyperfine splittings. These results demonstrated that the Mn-cluster is oxidized to the S_2 state with normal redox and magnetic properties in the presence of the chelator despite the loss of the carboxylate bands in the FTIR spectra. The results are interpreted as indicating that the chelator interacts with the Mn-cluster as a replacement of the native carboxylate ligand. This prevents the structural changes of the Mn-cluster and protein backbone which are induced upon the oxidation of the Mn-cluster up to the S_2 state, but preserve the redox and magnetic properties of the S_2 state Mn-cluster. The roles of Ca^{2+} in the photosynthetic oxygen evolution are also discussed.

Photosynthetic oxygen evolution is performed by an oxygen-evolving complex (OEC) in photosystem (PS)[1] II. The process involves the light-driven oxidation cycling through the five intermediate states which are labeled as S_n ($n = 0-4$) (*1*, *2*). The catalytic center of OEC comprises a tetranuclear manganese cluster located in the lumenal side of the D1 protein. The OEC is cumulatively oxidized by one equivalent for each step between the S_0 to S_4 states and is reduced during the S_4 to S_0 transition concurrent with the release of a molecular oxygen, although the Mn-cluster may not be directly oxidized for steps between the S_2 to S_4 states (reviewed in refs *3*−*7*). Both Ca^{2+} and Cl^- are involved as inorganic cofactors necessary for the catalytic activities for O_2 evolution (*3*). Recently, the X-ray crystallographic structure of the PS II protein complex was reported (*8*); however, the resolution was insufficient in providing details of the ligation structure of the Mn-cluster and did not shed much insight into the mechanism of water oxidation.

In recent years, FTIR spectroscopic studies, both in the mid-frequency region (2000−1000 cm^{-1}) and in the low-frequency region (1000−350 cm^{-1}), have been applied to examine the molecular structure of the Mn-cluster and the mechanism of O_2 evolution (reviewed in ref *9*). The S_2/S_1 FTIR difference spectrum in the mid-frequency region shows, in addition to the amide I and amide II bands, characteristic bands that correspond to the frequencies of carboxylate stretching vibrations (*10*−*16*, *28*). When carbon atom was uniformly labeled by ^{13}C, shifts in these bands were observed (*14*). The carboxylate bands have been ascribed to the carboxylate ligand associated with the Mn-cluster, although the amino acid residues responsible for the band formation are not determined (*17*). The appearance of the carboxylate

†This research was supported by grants for the Frontier Research System at RIKEN and Grant-in-Aid for Scientific Research (13640659) (to T.O.) from MECSST of Japan.

* To whom correspondence should be addressed. Tel: +81 (22) 228 2047. Fax: +81 (22) 228 2045. E-mail: ykimura@postman.riken.go.jp, takaaki@postman.riken.go.jp.

[1] Abbreviations: OEC, oxygen-evolving complex; PS, photosystem; Chl, chlorophyll; Q_A, primary quinone acceptor of photosystem II; Q_B, secondary quinone acceptor of photosystem II; Y_Z, redox active tyrosine of the D1 protein; Y_D, redox active tyrosine of the D2 protein; EXAFS, extended X-ray absorption fine structure; EPR, electron paramagnetic resonance; TL, thermoluminescence; FTIR, Fourier transform infrared; DCMU, 3-(3,4-dichlorophenyl)-1,1-dimethylurea; MES, 2-morpholinoethanesulfonic acid; EDTA, ethylenediamine-*N*,*N*,*N*′,*N*′-tetraacetic acid; EGTA, *O*,*O*′-bis(2-aminoethyl)ethyleneglycol-*N*,*N*,*N*′,*N*′-tetraacetic acid; Quin2, 8-amino-2-[(2-amino-5-methylphenoxy)methyl]-6-methoxyquinoline-*N*,*N*,*N*′,*N*′-tetraacetic acid, tetrapotassium salt.

10.1021/bi011216w CCC: $20.00
Published on Web 10/23/2001

bands in the different spectrum indicates that structural changes of the putative carboxylate ligand occur during the S_1 to S_2 transition. Two negative bands (1403 and 1560 cm^{-1}) with an energy difference of 157 cm^{-1} were assigned to the symmetric (ν_s) and the asymmetric (ν_{as}) stretching vibrations of the carboxylate in the S_1 state, respectively. Whereas, two positive bands (1364 and 1587 cm^{-1}) with an energy difference of 223 cm^{-1} were assigned to ν_s and ν_{as} modes of the carboxylate in the S_2 state, respectively. On the basis of the general criteria for the determination of the coordination structure in metal−ligand systems from the frequency difference $\Delta\nu$ ($= \nu_{as} - \nu_s$) between the asymmetric and the symmetric vibrational modes (*18*, *19*), it has been claimed that the carboxylate is in a bidentate coordination structure in the S_1 state and in an unidentate coordination structure in the S_2 state (*11*). Moreover, it has been proposed that the carboxylate serves as a bridge between the redox-active Mn ion and Ca^{2+} in the S_1 state, and since the carboxylate bands disappear in the Ca^{2+}-depleted membranes, the coordination bond between Ca^{2+} and the carboxylate is released upon the formation of the S_2 state (*11*). In contrast, previously reported S_2/S_1 spectra of the Sr^{2+}-supplemented PS II membranes did not indicate any shifts of the symmetric carboxylate band at 1404 cm^{-1} (*9*), thus reducing the likelihood of the bridging coordination model of the carboxylate between Ca^{2+} and the redox-active Mn.

The presence of Ca^{2+} in a close proximity to the Mn-cluster was demonstrated by Mn XAFS studies using native PS II membranes (*20*−*23*) and by Sr XAFS studies using the Sr^{2+}-substituted PS II membranes (*24*). Additionally, recent solid-state ^{113}Cd NMR studies of ^{113}Cd-substituted PS II membranes confirmed that Ca^{2+}-binding site is in the vicinity of the Mn-cluster, close enough to be affected by its electron spin state (*25*). In contrast, alterations in the Mn EXAFS Fourier peak at 3.3 Å were not detected when Ca^{2+} was replaced with Sr^{2+} or Dy^{3+}, suggesting that the distance between the Ca^{2+}-binding site and the Mn-cluster is further than 3.3 Å (*26*). Furthermore, EPR experiments for Mn^{2+}-supplemented PS II membranes indicated that the Ca^{2+}-site occupied by Mn^{2+} is located outside the first coordination sphere of the Mn-cluster (*27*).

The carboxylate stretching modes are prominent not only in the S_2/S_1 difference spectrum but also in the S_3/S_2 difference spectrum (*15*, *16*), although different carboxylate ligands may be responsible for each spectrum. Therefore, further studies of the carboxylate modes may provide insight toward understanding the molecular structure of the Mn-cluster and mechanism of O_2 evolution including the function of Ca^{2+}. In this paper, we report the behaviors of the carboxylate stretching bands in the light-induced S_2/S_1 FTIR difference spectrum of PS II membranes subjected to Ca^{2+} depletion and addition of chelating agents. In contrast to a previous report (*11*), our results showed that the effects of Ca^{2+} depletion on the characteristic S_2/S_1 difference vibrational structure, including the carboxylate bands, were insignificant. However, addition of exogenous chelating agent (EDTA or EGTA) markedly suppressed the light-induced spectral changes, despite not having any apparent effects on the redox property or magnetic structure of the Mn-cluster in the S_2 state. On the basis of these and other findings, possible ligation mode of the carboxylate residue to the Mn-cluster was proposed.

MATERIALS AND METHODS

Sample Preparations. BBY-type O_2-evolving PS II membranes (*29*) were prepared from spinach with modifications (*30*) and stored in liquid N_2 until use. After thawing the samples, the membranes were washed using a medium containing 400 mM sucrose, 20 mM NaCl, and 20 mM Mes/NaOH (pH 6.5) and then suspended in the same medium. For Ca^{2+} depletion, the membranes were suspended in a medium containing 2 M NaCl, 400 mM sucrose, and 20 mM Mes/NaOH (pH 6.5) at 0.5 mg of Chl/mL and treated at 0 °C for 25 min under weak light with gentle agitation. The following procedures were carried out under complete darkness or dim green light unless otherwise noted. Chelex 100 (100−200 mesh) was added to the membrane suspension (0.018 g of Chelex 100/1 mg of Chl) to remove any free Ca^{2+} ions from the suspension. The pH of the Chelex bed had been adjusted to pH 6.5 using HCl, followed by extensive washing using MILLI-Q water. After incubation at 0 °C for 10 min, the membranes were washed twice using a medium containing 400 mM sucrose (Sigma Ultra), 20 mM NaCl, and 20 mM Mes/NaOH (Aldrich 99.998%), pH 6.5 (medium A), in the presence of Chelex 100, and suspended in Chelex 100-treated medium A. The resulting Ca^{2+}-depleted membranes were further incubated at 0 °C for at least 3 h under complete darkness, and then stored in liquid N_2 until use. All wears for sample preparations were rinsed with acid before use.

The membrane samples for the FTIR measurements were suspended in Chelex-treated medium A (0.5 mg of Chl/mL). In the case where chelating agents or Ca^{2+} at the indicated concentration was added, the suspensions were further incubated at 0 °C for 5 min under darkness. Addition of Ca^{2+} was as chloride salt. DCMU was added to the suspension at 0.1 mM for the $S_2Q_A^-/S_1Q_A$ spectrum; 0.1 mM DCMU and 10 mM NH_2OH were added for the Q_A^-/Q_A spectrum. The membranes were precipitated by centrifugation for 30 min at 176000*g*, the resulting pellet was sandwiched between a pair of ZnSe disks. All sample manipulations for FTIR were performed under complete darkness with the use of a NightVision binocular (KOKUSEN D-2MV I) equipped with 800 nm cut-on filter. For EPR measurements, the membrane samples suspended in the Chelex-treated medium A (0.5 mg of Chl/mL) were supplemented with EDTA at the indicated concentration and 0.1 mM DCMU (50 mM dimethyl sulfoxide solution as stock). The membranes were precipitated by centrifugation, resuspended in the supernatant (approximately 4 mg of Chl/mL), and transferred to Spracil quartz EPR tubes.

Measurements. FTIR spectra were recorded on a vacuum-type spectrophotometer (Bruker IFS-66v/s) equipped with an MCT detector (EG&G OPTOELECTRONICS, J15D16-M204B−S01M-60-D316/6) and a cryostat (Oxford, Optistat DN1704) at 250 K. A custom-made CdTe band-pass filter (2000−350 cm^{-1}) was placed in front of the sample to eliminate the He−Ne laser scatter, which leaks from the interferometer compartment and to improve the signal-to-noise ratio. Sample temperature was controlled with a temperature controller (Oxford, ITC-502). For sample illumination, the cold light (HOYA-SCHOTT HL150R) passing through a long-path filter ($\geq$ 620 nm) was fed into the cryostat through a quartz window, which was placed in a

direction perpendicular to the monitoring light. Each single-beam spectrum was measured at 4 cm^{-1} resolution by averaging 300 scans (130 s accumulation). Four difference spectra in different samples were averaged to improve the signal-to-noise ratio.

Low-temperature X-band EPR spectra were measured using a Bruker E580 EPR spectrometer equipped with an Oxford-900 continuous flow cryostat with a temperature control system (Oxford, CF935). The membrane samples were illuminated from both sides at 250 K for 60 s using 650 W projectors.

Thermoluminescence was measured using a homemade apparatus. The membrane samples (0.25 mg of Chl/mL) were illuminated at 250 K with CW-light passing through a long-pass filter (≥ 630 nm) for 5 s and rapidly cooled in liquid N_2; the resulting light emission during warming was recorded (*30*). Each sample included 50 μM DCMU (dissolved in dimethyl sulfoxide as stock solutions) to ensure a single turnover from the S_1 to the S_2 state. Oxygen-evolving activity was measured at 25 °C using a Clark-type O_2 electrode in the presence of 0.25 mM phenyl-*p*-benzoquinone as an electron acceptor (*30*).

Ca^{2+} Determination. The concentrations of free Ca^{2+} in buffer solutions and sample suspensions were determined fluorometrically using a Ca^{2+}-sensitive fluorescence probe, Quin2. For the sample suspension, the Ca^{2+} amounts in the supernatant were determined after precipitating the membranes by centrifugation. Fluorescence of the Quin2−Ca^{2+} complex was measured at 500 nm with excitation at 339 nm (*31*, *32*) using a fluorescence spectrophotometer (HITACHI, F-4500).

RESULTS

Figure 1 shows the effects of Ca^{2+} depletion on the S_2/S_1 difference spectrum of PS II membranes. The S_2/S_1 spectra were obtained by subtracting the Q_A^-/Q_A difference spectrum from the $S_2Q_A^-/S_1Q_A$ difference spectrum after normalizing both $S_2Q_A^-/S_1Q_A$ and Q_A^-/Q_A spectrum with respect to the intensity of the CO stretching band of Q_A^- at 1479 cm^{-1}. DCMU was added for the $S_2Q_A^-/S_1Q_A$ spectrum as an inhibitor of the electron transfer from Q_A to Q_B. NH_2OH and DCMU were added for the Q_A^-/Q_A spectrum as an exogenous electron donor and as the inhibitor, respectively (*10*, *33*). The double difference spectrum of the nontreated control PS II membranes showed the characteristic vibrational feature of the S_2/S_1 difference spectra at 1365(+)/1404(−) cm^{-1} for the symmetric and at 1587(+)/1562(−) cm^{-1} for the asymmetric stretching vibrations of the carboxylate ligand for the Mn-cluster. Additionally, the spectrum showed the pronounced differential bands appearing in the 1690−1630 cm^{-1} (amide I) and 1590−1515 cm^{-1} (amide II) regions, which correspond to the conformational change of the backbone protein upon the S_1 to S_2 transition (Figure 1a). The present double difference spectrum closely resembles the single-pulse induced S_2/S_1 spectrum of the nontreated membranes in the presence of ferricyanide/ferrocyanide (*11*, *12*). It has been previously reported that the carboxylate stretching bands disappear from the spectrum of the membranes that were depleted of Ca^{2+} using low-pH treatment (*11*). To the contrary, as shown in Figure 1b, the carboxylate bands were decisively evident in our Ca^{2+}-depleted membranes, although the O_2-evolving activity was inhibited in the depleted membranes as shown in Table 1. Replenishment of Ca^{2+} restored the inhibited O_2 evolution (up to 80%) but did not affect the carboxylate bands (Figure 1c). The amide I and II bands were somewhat modified by Ca^{2+} depletion but were not restored by the replenishment of Ca^{2+} (Figure 1c). Therefore, these changes can be attributed to some anomalous effects induced by the high-salt washing. It is of note that overlapping large absorption bands due to the backbone protein matrixes and the presence of water create difficulties in allowing detailed analyses of the spectra.

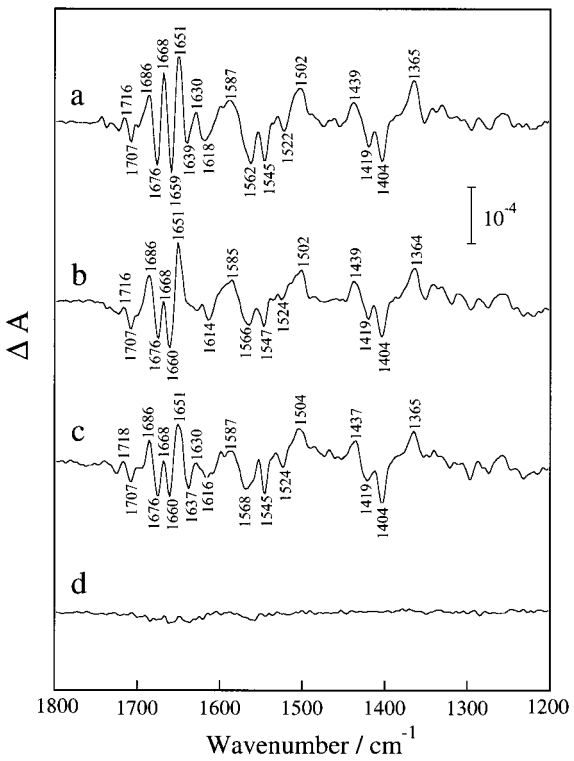

FIGURE 1: Light-induced S_2/S_1 difference spectra of PS II membranes that are (a) untreated, (b) Ca^{2+}-depleted, and (c) Ca^{2+}-replenished. For Ca^{2+} replenishment (c), Ca^{2+}-depleted sample membranes were supplemented with 20 mM $CaCl_2$ and incubated at 0 °C for 5 min. Each S_2/S_1 difference spectrum was obtained by subtracting the Q_A^-/Q_A difference spectrum from the $S_2Q_A^-/S_1Q_A$ difference spectrum (see text for details). Membrane samples were illuminated with continuous light (2 mW/cm^2) at 250 K for 10 s. Sample suspension included 0.1 mM DCMU for the $S_2Q_A^-/S_1Q_A$ difference spectrum, or 0.1 mM DCMU and 10 mM NH_2OH for the Q_A^-/Q_A difference spectrum. A dark minus dark FTIR spectrum (d) was presented to show a noise level.

Table 1: Effects of Addition of Ca^{2+} or EDTA on the O_2-Evolving Activity

PSII membrane	O_2-evolving activity μmol of O_2 (mg of Chl)$^{-1}$ h^{-1}		
	no addition	+20 mM $CaCl_2$	+1 mM EDTA
nontreated	602 (93)[a]	646 (100)	602 (93)
NaCl/light-treated	105 (16)	521 (81)	106 (16)

[a] Numbers in parentheses represent the oxygen-evolving activity in relative %.

Figure 2 shows the S_2/S_1 difference spectra of the Ca^{2+}-depleted PS II membranes with (a) no-addition, (b) addition of 1 mM EDTA, (c) addition of 1 mM EGTA, and (d) addition of 1 mM EDTA followed by 20 mM $CaCl_2$. As

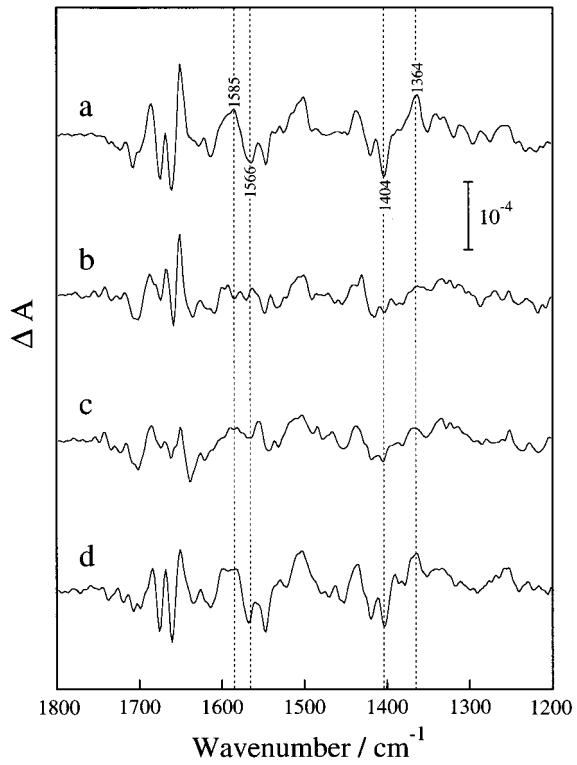

FIGURE 2: Light-induced S_2/S_1 difference spectra showing the effects of chelating agents on Ca^{2+}-depleted PS II membranes with (a) no-addition, (b) addition of 1 mM EDTA, (c) addition of 1 mM EGTA, and (d) addition of 1 mM EDTA followed by 20 mM $CaCl_2$. For (d), the membranes were incubated with 1 mM EDTA at 0 °C for 5 min, then 20 mM $CaCl_2$ was added. Each S_2/S_1 difference spectrum was obtained by subtracting the Q_A^-/Q_A difference spectrum from the $S_2Q_A^-/S_1Q_A$ difference spectrum (see text for details). Membrane samples were illuminated with continuous light (2 mW/cm^2) at 250 K for 10 s. Sample suspension included 0.1 mM DCMU for the $S_2Q_A^-/S_1Q_A$ difference spectrum, or 0.1 mM DCMU and 10 mM NH_2OH for the Q_A^-/Q_A difference spectrum.

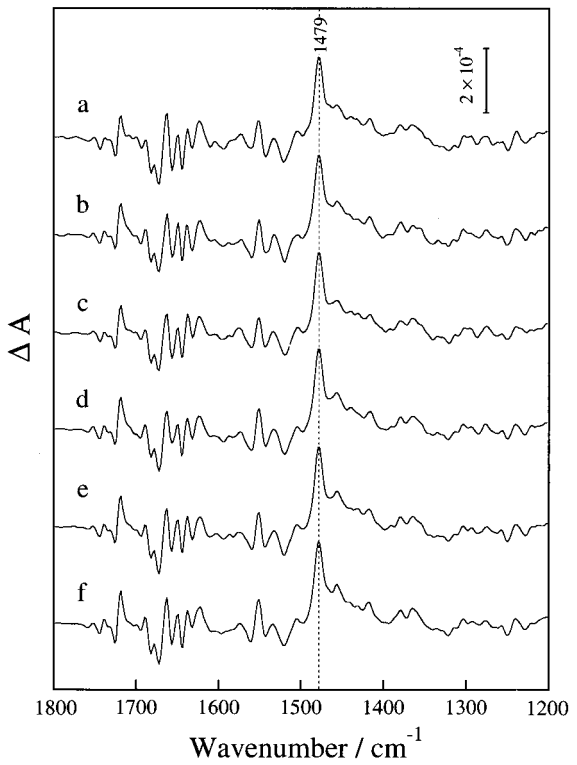

FIGURE 3: Light-induced Q_A^-/Q_A difference spectra of (a) untreated PS II membranes with 20 mM $CaCl_2$, and Ca^{2+}-depleted PS II membranes with (b) no-addition, (c) addition of 20 mM $CaCl_2$, (d) addition of 1 mM EDTA, (e) addition of 1 mM EGTA, and (f) addition of 1 mM EDTA followed by 20 mM $CaCl_2$. Each spectrum was normalized with respect to the intensity of the Q_A^- band at 1479 cm^{-1}. Membrane samples were illuminated with continuous light (2 mW/cm^2) at 250 K for 10 s. Sample suspension included 0.1 mM DCMU and 10 mM NH_2OH.

shown in Figure 2b, addition of 1 mM EDTA significantly affected the typical features of the S_2/S_1 spectrum; in particular, the carboxylate bands at 1364(+)/1404(−) cm^{-1} for symmetric and 1585(+)/1566(−) cm^{-1} for asymmetric vibrations disappeared concomitant with considerable abolishment of the bands in the amide I and II regions. Similar effects were observed for the spectrum of the sample supplemented with 1 mM EGTA (Figure 2c), and it can be suggested that the chelating functions of these chemicals are responsible for their effects on the spectra. Small carboxylate bands that were observed in the EDTA- and EGTA-supplemented spectra can be explained as the residual Ca^{2+}-retaining PS II fraction surviving the treatments for Ca^{2+} depletion (see Table 1). In contrast to the carboxylate stretching bands, the chelators did not affect the bands in the 1750−1700 cm^{-1} region due to carbonyl-stretching ν(CO) modes for protonated acidic amino acid residues (*15*). The characteristic S_2/S_1 vibrational structure, including the amide I and II bands, which disappeared with the addition of 1 mM EDTA, were recovered by the subsequent replenishment with 20 mM Ca^{2+} (Figure 2d). It should be noted that these effects, which result from the addition of the chelator, were observed only for the sample subjected to Ca^{2+} depletion, since no spectral changes were induced by the chelator in the nontreated control membranes (data not shown).

Figure 3 shows effects of Ca^{2+} depletion and the following addition of a chelator on the Q_A^-/Q_A difference spectra. It was evident that the variously treated membrane samples provided very similar Q_A^-/Q_A spectra; in particular, changes were not observed for the amide I and II bands, of which formation was significantly inhibited by the chelator in the S_2/S_1 difference spectrum. These results indicate that Q_A and its surrounding protein structure are not affected by these treatments. Therefore, the acceptor side of PS II does not contribute to the changes of the S_2/S_1 double difference spectrum induced by Ca^{2+} depletion and chelator.

Figure 4 shows the effect of EDTA concentration of the medium on the suppression of the band intensity of the symmetric carboxylate stretching vibration at 1404 cm^{-1} in Ca^{2+}-depleted PS II membranes. The intensities of the negative band at 1404 cm^{-1} in the $S_2Q_A^-/S_1Q_A$ spectrum (shown in the inset figure) were plotted as a function of the EDTA concentration. Evaluation of the band intensities using the $S_2Q_A^-/S_1Q_A$ difference spectra afforded a higher precision than using the double difference spectra. The band intensities at 1404 cm^{-1} decreased with EDTA concentration to reach the low plateau level at 1 mM EDTA. The residual band intensities at the higher EDTA concentrations were due to the nondepleted PS II fraction present in the Ca^{2+}-depleted membrane samples and to the small contribution of Q_A^-/Q_A spectrum at this wavenumber. If we assumed that EDTA is

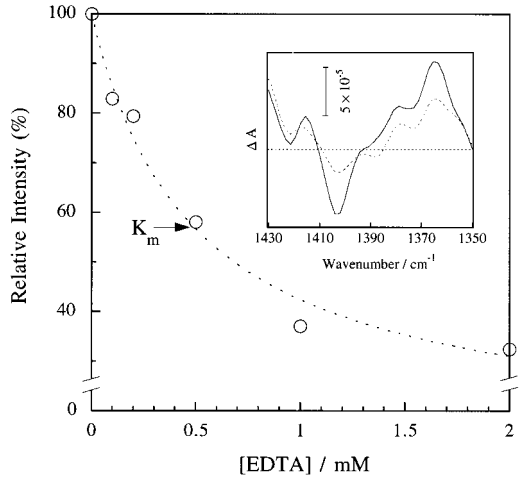

FIGURE 4: Relationship between EDTA concentration and the disappearance of the symmetric carboxylate band at 1404 cm^{-1} for Ca^{2+}-depleted PS II membranes. Intensities of the symmetric carboxylate bands were estimated using the negative band at 1404 cm^{-1} in the $S_2Q_A^-/S_1Q_A$ difference spectra since contribution of Q_A^-/Q_A bands is minimal at this wavenumber (see text for details). Each $S_2Q_A^-/S_1Q_A$ difference spectrum was normalized with respect to the intensity of the Q_A^- band at 1479 cm^{-1}. The apparent K_d value of 0.49 mM was calculated from the dashed curve, which was fitted over the experimental data. Inset shows the $S_2Q_A^-/S_1Q_A$ difference spectra in the absence (solid line) and in the presence of 1 mM EDTA (dashed line). For other experimental conditions, see the legend in Figure 1.

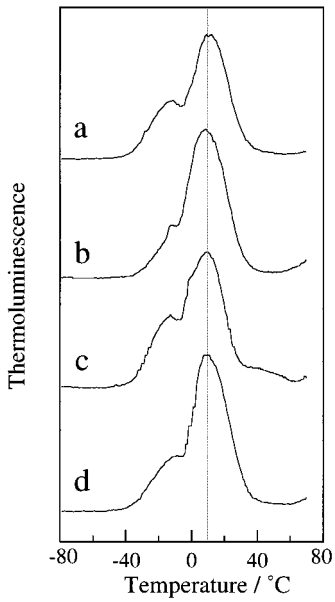

FIGURE 5: Thermoluminescence glow curves for Ca^{2+}-depleted PS II membranes with (a) no-addition, (b) addition of 20 mM $CaCl_2$, (c) addition of 1 mM EDTA, and (d) addition of 1 mM EDTA followed by 20 mM $CaCl_2$. Membrane samples (250 μg of Chl/mL) were illuminated with continuous light at 250 K for 5 s. Sample suspension included 0.1 mM DCMU. The small shoulder at approximately 0 °C is an artifact due to the influence of melting ice on the heating rate.

associated to the OEC in interrupting the generation of the S_2/S_1 bands, the apparent dissociation constant was calculated as 0.49 mM.

One possible suggestion to explain the effect of the chelators is simply their capacity to eliminate the free Ca^{2+} ions that contaminate in the sample suspension; the contaminated Ca^{2+} is bound to the Ca^{2+} site to restore the normal S_2/S_1 spectrum in the absence of a chelator. However, this was apparently not the case since Ca^{2+} quantification in the buffer mediums and in the sample suspension for FTIR measurements showed that the Ca^{2+} concentration was lower than the detectable limit (<0.2 μM) of the Ca^{2+}-sensitive fluorescence probe. The value was significantly lower than the EDTA concentration required for the suppression of the FTIR band formations that are shown in Figure 4. We also examined the possibility of Ca^{2+} contamination during the FTIR measurements, and the result indicated that release of Ca^{2+} (<0.2 μM) to the reaction medium that was sandwiched between ZnSe disks was not detected even after incubation for 2 h at room temperature. These results clearly demonstrated that the effects of the chelators are not simply due to the elimination of free Ca^{2+} in the sample suspension.

Figure 5 shows the effect of Ca^{2+} depletion and chelator addition on the TL glow curves of Ca^{2+}-depleted PS II membranes. Sample membranes were illuminated with CW-light at 250 K in the presence of 50 μM DCMU, which ensured a single turnover of PS II from the S_1 to the S_2 state. Sample membranes that were Ca^{2+}-depleted, EDTA-supplemented, and Ca^{2+}-replenished showed the same TL Q-band arising from the charge recombination of an $S_2Q_A^-$ charge pair (*34*). The results indicated that the S_2 state formed in the Ca^{2+}-depleted membranes retains the normal redox properties. We did not detect any effects on the S_2 properties and the yield of S_2-formation from the presence of a chelator,

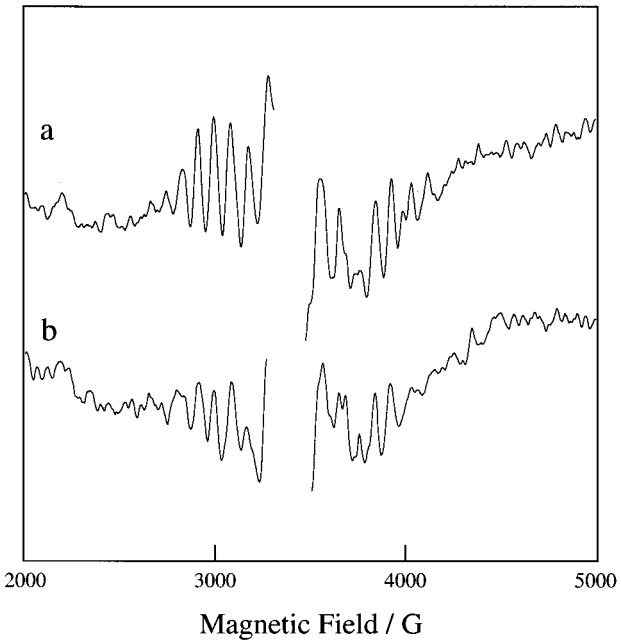

FIGURE 6: S_2 EPR multiline spectra (light minus dark) in Ca^{2+}-depleted PS II membranes with (a) no addition and (b) addition of 1 mM EDTA. Membrane samples were illuminated with continuous light at 250 K for 1 min. Sample suspension included 0.1 mM DCMU. Instrument settings were temperature, 6 K; microwave power, 0.2 mW; microwave frequency, 9.5 GHz; modulation frequency and amplitude, 100 kHz and 15 G, respectively.

even though the chelator resulted in marked modifications in the S_2/S_1 vibrational structure.

Figure 6 shows the EPR spectra of the Ca^{2+}-depleted PS II membranes (light minus dark). A sample suspension including 0.1 mM DCMU was illuminated with continuous light at 250 K to allow only the S_1 to S_2 transition. The Ca^{2+}-

depleted membranes without EDTA supplementation generated a multiline S_2 signal (Figure 6a) with spectral features that were indistinguishable from those observed for the nontreated control membranes. The S_2 multiline signal of EDTA-supplemented membranes (Figure 6b) was also similar, although its signal intensities were relatively weaker. These results are compatible with the previous report that the normal multiline signal was generated by the illumination of the Ca^{2+}-depleted membranes in the presence of EGTA at 198 K, which is the temperature that interrupts further transition beyond the S_2 state, while the dark-stable modified multiline signal was induced when the Ca^{2+}-depleted membranes were illuminated at 0 °C in the absence of DCMU to produce the $S_2Y_Z^+$ state, followed by dark-decay to the S_2-state (*39*). The reason for the relatively lower multiline amplitude in the presence of EDTA is not clear at present, but might be attributable to the presence of the minor OEC fraction which shows no multiline in the presence of EDTA or the change in the signal saturation characteristics reported previously by Boussac et al. (*37*, *39*). A $g = 4$ S_2 signal was not induced in the Ca^{2+}-depleted membranes with and without EDTA, and was not restored by Ca^{2+}-replenishment (data not shown). The results indicate that the magnetic structure of the S_2 state Mn-cluster is normal in both Ca^{2+}-depleted and EDTA-supplemented membranes, and that the addition of EDTA did not induce any specific modification of the magnetic structure.

DISCUSSION

Effects of Ca^{2+} Depletion. The S_2/S_1 difference spectrum of the low-pH induced Ca^{2+}-depleted PS II membranes indicated that the symmetric (1364(+)/1403(−) cm^{-1}) and the asymmetric (1589(+)/1561(−) cm^{-1}) stretching bands of the carboxylates were not generated with the appearance of no new bands corresponding to them as reported (*11*). The carboxylate bands were subsequently almost completely restored by the replenishment of Ca^{2+}. On the basis of the Ca^{2+}-dependence and the frequency difference between the asymmetric and symmetric vibrational modes, it was proposed that a carboxylate bridging between the redox-active Mn and Ca^{2+} was responsible for the FTIR bands and the coordination mode of the carboxylate changed from the bidentate to the unidentate structure in the S_1 to S_2 transition (*11*). However, our present study clearly demonstrates that Ca^{2+} depletion does not affect the carboxylate stretching bands in the S_2/S_1 spectrum, indicating that the putative carboxylate bridging between Ca and Mn is not responsible for the carboxylate bands found in the S_2/S_1 spectrum. Our observations are consistent with the finding that Sr^{2+} substitution did not induce any changes of the carboxylate bands in the S_2/S_1 spectrum (ref *9* and unpublished results). We should emphasize within this context that EDTA was always included in the sample suspension of the Ca^{2+}-depleted membranes in the previous study (*11*). In addition, the sample suspension of the previous study included 78 mM potassium ions as potassium ferrocyanide and potassium ferricyanide which were used for electron acceptor and redox buffer. K^+ was found to be bound to the Ca^{2+}-site to suppress the S_2/S_1 bands (unpublished data). Therefore, the absence of the carboxylate bands in the previous study is probably caused by the presence of both EDTA and K^+, although we cannot completely exclude the effects of the presence of the extrinsic proteins in the low-pH induced Ca^{2+}-depleted membranes and/or difference in the procedures for Ca^{2+}-depletion. If we reconsider, in the light of our present results, the change in the ligation mode of the carboxylate ligand from bidentate to unidentate upon the S_1 to S_2 transition, we can propose that the carboxylate bridges between two Mn ions or, alternatively, chelates one Mn ion in bidentate manner in the S_1 state. However, we cannot distinguish these two types of bidentate structure by the values for the frequency difference $\Delta\nu$ ($= \nu_{as} - \nu_s$) between the asymmetric and the symmetric vibrational modes because $\Delta\nu$ largely depends on the ligands (*18*, *19*, *35*). Then, one of the coordination bonds is selectively released to cause the appearance of the unidentate structure upon S_2 formation. This coordination change may facilitate the binding of substrate water to the Mn-cluster.

As shown in Figure 1, significant differences were not observed for the S_2/S_1 spectra of the Ca^{2+}-depleted membranes before and after Ca^{2+} replenishment, which restored O_2 evolution. The structural changes of the protein matrixes that were induced by the oxidation of the Mn-cluster proceeded almost normally in the absence of Ca^{2+}. Therefore, it is likely that the ligation structure of the Mn-cluster and the protein conformation in the vicinity of the cluster in the absence of Ca^{2+} are comparable to those in the presence of Ca^{2+}, in both the S_2 and S_1 states. Furthermore, the redox and magnetic properties of the S_2 state Mn-cluster in the absence of Ca^{2+} are indistinguishable from those of the normal S_2 state as indicated by their $S_2Q_A^-$ TL band (Figure 5) and their S_2 state multiline EPR signal with normal hyperfine structure (Figure 6). To summarize, the Mn-cluster in the Ca^{2+}-depleted and native PS II membranes has inherently identical properties in the S_1 and S_2 states, except for the inhibition of O_2-evolving capability. This suggests that Ca^{2+} is not directly involved in the structural changes of OEC induced by the oxidation of the Mn-cluster during the S_1 to S_2 transition, and therefore, Ca^{2+} is likely to play key roles, in states higher than S_2, which control the ligation structure and redox chemistry of the Mn-cluster necessary for the oxygen evolution as well as the binding of the substrate water. Chu et al. (*36*) have reported that Sr^{2+}-substitution affects the vibrational mode at 606 cm^{-1}, which is tentatively assigned to a Mn−O−Mn cluster mode. This Sr^{2+}-dependent change of the 606 cm^{-1} mode may be compatible with the formation of the modified multiline S_2 signal in the substituted membranes (*37*, *38*). FTIR studies in the low-frequency region for the Ca^{2+}-depleted samples, which were used in the present study, may provide further insight into the mechanism of water oxidation and Ca^{2+} function in OEC.

Effects of Chelating Agents. Light-induced changes in the FTIR spectra upon the S_1 to S_2 transition were largely suppressed by the addition of EDTA or EGTA to the Ca^{2+}-depleted PS II membranes without appearance of any new band, as shown in Figure 2. The absence of the FTIR bands cannot be explained as the interruption of the S_2 formation by the chelator, since the S_2 formation was demonstrated by the generation of the $S_2Q_A^-$ TL band and by the multiline S_2 signal, as shown in Figures 5 and 6, respectively. The band intensities of the FTIR spectra obtained in the present experimental conditions were not affected by halving the S_2

acquisition time and by doubling the illumination time. Furthermore, the yield of the S_2 formation as measured by TL at various temperatures was not affected by the presence of EDTA (unpublished data). These show that the disappearance of the S_2/S_1 vibrational modes by the chelator is not attributed to an insufficient S_2 formation due to a lower quantum yield of the S_2 formation or a shorter lifetime of the S_2 state. The chelators did not inhibit the generation of the S_2/S_1 bands for the nontreated control membranes. Therefore, the effects of the chelator may not be caused by nonspecific interaction between the carboxylic groups of the chelator and amino acid residues of OEC. Although the details on the action of the chelator remain to be resolved, we present one possible explanation, which involves the association between the chelator(s) and the Mn-cluster. The association of chelators to the Mn-cluster was previously suggested for Ca^{2+}-depleted membranes by CW (*37*, *39*) and pulsed EPR (*40*). The presence of a chelator has induced the formation of the dark-stable modified S_2 multiline signal when Ca^{2+}-depleted membranes were illuminated at 0 °C to produce the $S_2Y_Z^+$ state in the absence of DCMU. The binding of EGTA to a close vicinity of the Mn-cluster is suggested from the ESEEM data for the Ca^{2+}-depleted membranes obtained from ^{14}N- and ^{15}N-labeled material (*40*). Within this context, it is of note that association between a high-concentration adventitious carboxylic acid, such as citrate, and the Mn-cluster has been suggested by EPR study (*39*). Our FTIR results indicated that the chelators interact with the Mn-cluster at the S_1 and/or S_2 states, because DCMU was always included in the sample suspension. It is clear that such associations do not significantly influence the magnetic properties of the cluster. Therefore, the mode of interaction between the chelators and the Mn-cluster detected by FTIR may be rather different than those reported by EPR studies. Consistent with this view, the addition of citrate (~40 mM) did not influence the S_2/S_1 spectrum of the Ca^{2+}-depleted membranes (data not shown).

On the basis of these considerations, we propose that a chelator interacts with the Mn-cluster as a replacement for the native carboxylate ligand responsible for the generation of the carboxylate stretching bands. In nontreated control membranes, neither O_2-evolving capability nor S_2/S_1 spectra were influenced by the chelator (data not shown), indicating that Ca^{2+}-binding interferes with either the access of the chelators to the Mn-cluster, the replacement of the native carboxylate ligand by adventitious carboxylate groups, or both. Since the carboxylate stretching bands were not induced in the chelator-supplemented membranes, the S_1 to S_2 transition was not accompanied by the change of the ligation mode of the chelator. The presence of chelator(s) suppressed the generation of not only the carboxylate stretching bands but also the amide I and II bands, which indicate the structural changes of the protein matrixes upon the oxidation of the Mn-cluster. Therefore, we conclude that the native carboxylate ligand is crucial for inducing the changes of the structure of protein and/or the hydrogen bonding to the peptide backbone during the oxidation of the Mn-cluster. The formation of the normal S_2 multiline signal and the normal $S_2Q_A^-$ TL band in the EDTA-supplemented membranes suggests that the redox and magnetic properties of the S_2 state Mn-cluster are largely normal in the chelator-supplemented membranes. Therefore, the ligation geometry of the Mn-cluster in the S_2 state may not be significantly affected due to the presence of the chelators, and if this is the case, the chelator carboxylate may be associated in an unidentate manner with the Mn-cluster in the S_1 state. Alternatively, the chelator may be associated in a bidentate manner with the Mn-cluster after the formation of the S_2 state; however, such association would not influence the redox and magnetic properties of the S_2 state cluster. Both oxygen and nitrogen atoms of EDTA or EGTA participate in the formation of a stable chelating complex with a metal cation. Therefore, the nitrogen atom may also be involved in the association between EDTA or EGTA and the Mn-cluster. Furthermore, although supporting experimental data has not yet been reported, we cannot exclude the possibility that the chelator is not associated directly with the Mn-cluster, but is bound within a close proximity to the cluster to perturb the proper structure of the native carboxylate ligand.

Our discussion is based on the assumption that the carboxylate stretching bands in the S_2/S_1 spectrum reflect the alteration of the ligation structure of the carboxylate ligand. It has been suggested that the frequency difference ($\Delta\nu$) between the asymmetric and symmetric carboxylate stretching vibrations observed in the S_2/S_1 spectrum may be caused by the valence change of the Mn ion, without any changes in the ligation structure, since the oxo-bridged Mn carboxylate complexes showed various $\Delta\nu$ depending on their oxidation states (*41*). However, we find it difficult to apply this view into explaining our present observation, in which the carboxylate stretching bands were markedly suppressed despite the normal progress of the oxidation of the Mn-cluster. Additionally, the frequency difference observed in the model complexes with bidentate bridging ligands increased with the reduction of Mn, which contradicts the tendency of the change in the S_2/S_1 spectra. Therefore, it is likely that the change in the oxidation state of the Mn-cluster itself does not contribute significantly to either the formation of the carboxylate bands or the observed frequency difference between the S_1 and S_2 states.

ACKNOWLEDGMENT

We are thankful to Dr. H. Mino for the kind help during the EPR measurements. We also thank Dr. T. Noguchi for valuable advice for the FTIR measurements.

REFERENCES

1. Joliot, P., Barbieri, G., and Chabaud, R. (1969) *Photochem. Photobiol. 10*, 309−329.
2. Kok, B., Forbush, B., and McGloin, M. (1970) *Photochem. Photobiol. 11*, 457−475.
3. Debus, R. J. (1992) *Biochim. Biophys. Acta 1102*, 269−352.
4. Hoganson, C. W., and Babcock, G. T. (2000) *Met. Ions Biol. Syst. 37*, 613−656.
5. Robblee, J. H., Cinco, R. M., and Yachandra, V. K. (2001) *Biochim. Biophys. Acta 1503*, 7−23.
6. Geijer, P., Peterson, S., Åhrling, K. A., Deák, Z., and Styring, S. (2001) *Biochim. Biophys. Acta 1503*, 83−95.
7. Renger, G. (2001) *Biochim. Biophys. Acta 1503*, 210−228.
8. Zouni, A., Witt, H.-T., Kern, J., Fromme, P., Krauss, N., Saenger, W., and Orth, P. (2001) *Nature 409*, 739−743.
9. Chu, H.-A., Hillier, W., Law, N. A., and Babcock, G. T. (2001) *Biochim. Biophys. Acta 1503*, 69−82.

10. Noguchi, T., Ono, T.-A., and Inoue, Y. (1992) *Biochemistry 31*, 5953−5956.
11. Noguchi, T., Ono, T.-A., and Inoue, Y. (1995) *Biochim. Biophys. Acta 1228*, 189−200.
12. Noguchi, T., Ono, T.-A., and Inoue, Y. (1995) *Biochim. Biophys. Acta 1232*, 59−66.
13. Zhang, H., Fischer, G., and Wydrzynski, T. (1998) *Biochemistry 37*, 5511−5517.
14. Noguchi, T., Sugiura, M., and Inoue, Y. (1999) in *Fourier Transform Spectroscopy* (Itoh, K., and Tasumi, M., Eds.) pp 459−460, Waseda University Press, Tokyo, Japan.
15. Noguchi, T., and Sugiura, M. (2001) *Biochemistry 40*, 1497−1502.
16. Hillier, W., and Babcock, G. T. (2001) *Biochemistry 40*, 1503−1509.
17. Chu, H.-A., Debus, R. J., and Babcock, G. T. (2001) *Biochemistry 40*, 2312−2316.
18. Deacon, G. B., and Phillips, R. J. (1980) *Coord. Chem. Rev. 33*, 227−250.
19. Nakamoto, K. *(1986) Infrared and Raman Spectra of Inorganic and Coordination Compounds*, pp 231−233, Wiley, New York.
20. Yachandra, V. K., DeRose, V. J., Latimer, M. J., Mukerji, I., Sauer, K., and Klein, M. P. (1993) *Science 260*, 675−679.
21. Latimer, M. J., DeRose, V. J., Mukerji, I., Yachandra, V. K., Sauer, K., and Klein, M. P. (1995) *Biochemistry 34*, 10898−10909.
22. Yachandra, V. K., Sauer, K., and Klein, M. P. (1996) *Chem. Rev. 96*, 2927−2950.
23. Latimer, M. J., DeRose, V. J., Yachandra, V. K., Sauer, K., and Klein, M. P. (1998) *J. Phys. Chem. B 102*, 8257−8265.
24. Cinco, R. M., Robblee, J. H., Rompel, A., Fernandez, C., Yachandra, V. K., Sauer, K., and Klein, M. P. (1998) *J. Phys. Chem. B 102*, 8248−8256.
25. Matysik, J., Nachtegaal, G., van Gorkom, H. J., Hoff, A. J., and de Groot, H. J. M. (2000) *Biochemistry 39*, 6751−6755.
26. Riggs-Gelasco, P. J., Mei, R., Ghanotakis, D. F., Yocum, C. F., and Penner-Hahn, J. E. (1996) *J. Am. Chem. Soc. 118*, 2400−2410.
27. Booth, P. J., Rutherford, A. W., and Boussac, A. (1996) *Biochim. Biophys. Acta 1277*, 127−134.
28. Chu, H.-A., Hillier, W., Law, N. A., Sackett, H., Haymond, S., and Babcock, G. T. (2000) *Biochim. Biophys. Acta 1459*, 528−532.
29. Berthold, D. A., Babcock, G. T., and Yocum, C. F. (1981) *FEBS Lett. 134*, 231−234.
30. Ono, T.-A., and Inoue, Y. (1986) *Biochim. Biophys. Acta 850*, 380−389.
31. Tsien, R. Y. (1981) *Nature 290*, 527−528.
32. Miyoshi, N., Hara, K., Kimura, S., Nakanishi, K., and Fukuda, M. (1991) *Photochem. Photobiol. 53*, 415−418.
33. Berthomieu, C., Nabedryk, E., Mäntele, W., and Breton, J. (1990) *FEBS Lett. 269*, 363−367.
34. Rutherford, A. W., Crofts, A. R., and Inoue, Y. (1982) *Biochim. Biophys. Acta 682*, 457−465.
35. Socrates, G. (1994) *Infrared Characteristic Group Frequencies*, 2nd ed.; Wiley, Chichester.
36. Chu, H.-A., Sackett, H., and Babcock, G. T. (2000) *Biochemistry 39*, 14371−14376.
37. Boussac, A., and Rutherford, A. W. (1988) *Biochemistry 27*, 3476−3483.
38. Boussac, A., Zimmermann, J.-L., and Rutherford, A. W. (1989) *Biochemistry 28*, 8984−8989.
39. Boussac, A., Zimmermann, J.-L., and Rutherford, A. W. (1990) *FEBS Lett. 277*, 69−74.
40. Zimmermann, J.-L., Boussac, A., and Rutherford, A. W. (1993) *Biochemistry 32*, 4831−4841.
41. Smith, J. C., Gonzalez-Vergara, E., and Vincent, J. B (1997) *Inorg. Chim. Acta 255*, 99−103.

BI011216W